

DARK MATTER HALO ASSEMBLY BIAS: ENVIRONMENTAL DEPENDENCE IN THE NON-MARKOVIAN EXCURSION SET THEORY

JUN ZHANG

Center for Astronomy and Astrophysics, Department of Physics and Astronomy, Shanghai Jiao Tong University, 955 Jianchuan road, Shanghai, 200240, China

CHUNG-PEI MA

Department of Astronomy, University of California, Berkeley, CA 94720, USA

ANTONIO RIOTTO

Department of Theoretical Physics and Center for Astroparticle Physics (CAP), 24 quai E. Ansermet, CH-1211 Geneva, Switzerland

Draft version October 30, 2018

ABSTRACT

In the standard excursion set model for the growth of structure, the statistical properties of halos are governed by the halo mass and are independent of the larger scale environment in which the halos reside. Numerical simulations, however, have found the spatial distributions of halos to depend not only on their mass but also on the details of their assembly history and environment. Here we present a theoretical framework for incorporating this “assembly bias” into the excursion set model. Our derivations are based on modifications of the path integral approach of Maggiore & Riotto (2010) that models halo formation as a non-Markovian random walk process. The perturbed density field is assumed to evolve stochastically with the smoothing scale and exhibits correlated walks in the presence of a density barrier. We write down conditional probabilities for multiple barrier crossings, and derive from them analytic expressions for descendant and progenitor halo mass functions and halo merger rates as a function of both halo mass and the linear overdensity δ_e of the larger-scale environment of the halo. Our results predict a higher halo merger rate and higher progenitor halo mass function in regions of higher overdensity, consistent with the behavior seen in N -body simulations.

Subject headings: general - cosmology: theory - galaxies: halos - galaxies: clustering - dark matter

1. INTRODUCTION

In hierarchical cosmological models such as Λ CDM, dark matter halos of lower mass form earlier on average than more massive halos. The virial mass of halos is a key parameter that governs many properties of galaxies and their host halos, e.g., galaxy morphology and color, baryonic feedback processes, formation redshift, and halo occupation number. Recent numerical simulations, however, have shown that a halo’s local environment – in addition to its mass – also affects the formation processes. At a *fixed* mass, older halos are found to cluster more strongly than more recently formed halos (Gottlöber et al. 2001; Sheth & Tormen 2004; Gao et al. 2005; Harker et al. 2006; Wechsler et al. 2006; Jing et al. 2007; Wang et al. 2007; Gao & White 2007; Maulbetsch et al. 2007; Angulo et al. 2008; Dalal et al. 2008; Li et al. 2008). Other halo properties such as concentration, spin, shape, velocity structure, substructure mass function, merger rates, and halo occupation distribution have also been shown to vary with halo environment (e.g., Avila-Reese et al. 2005; Wechsler et al. 2006; Jing et al. 2007; Gao & White 2007; Bett et al. 2007; Wetzel et al. 2007; Fakhouri & Ma 2009, 2010; Faltenbacher & White 2010; Zentner et al. 2013).

In comparison, the formation and properties of dark matter halos depend only on the mass and not environment in the extended Press-Schechter and excursion set models (Press & Schechter 1974; Bond et al. 1991; Lacey

& Cole 1993). These models are used widely for making theoretical predictions of halo and galaxy statistics and for Monte Carlo constructions of merger trees. The lack of environmental correlation arises from the Markovian nature of the random walks in the excursion set model: the change of the matter over-density as a function of the smoothing scale is treated as a Markovian process, which by definition decouples the density fluctuations on small (halo) and large (environment) scales. This limitation stems from the use of the Fourier-space tophat window function as the mass filter. When a Gaussian window function is used, for instance, Zentner (2007) finds an environmental dependence in the halo formation redshift, but the dependence is *opposite* to that seen in the numerical simulations cited above. Several other attempts at incorporating environmental effects into the excursion set model were not able to reproduce the correlations seen in the simulations (e.g., Sandvik et al. 2007; Desjacques 2008).

In this paper we aim to derive analytic expressions for halo statistics that depend on halo mass as well as its large-scale environmental density. To achieve this goal, we begin with the non-Markovian extension of the excursion set model by Maggiore & Riotto (2010a) (MR10 hereafter). In this approach, a path integral formalism is used to perform perturbative calculations for non-Markovian processes of Gaussian fields. A key quantity is the probability that the smoothed matter over-density remains below a critical value down to a certain mass scale

(equation [40] of MR10). They show that this quantity can be written as a multi-variable integral of a Gaussian distribution function, which can be worked out exactly in the Markovian case, and perturbatively for weakly non-Markovian processes (see §3, 4, 5 of MR10 for details). This probability can be used to derive the first-crossing rate for the halo mass function as shown in equation (42) of MR10.

To introduce environmental dependence, we modify equation (40) of MR10 by first isolating (*i.e.*, not integrating out) the dependence of the matter overdensity on the specified environmental scale in this equation. We then add to the path integral a portion that is between the descendant and progenitor halo mass scales with a slightly higher critical value for halo identification (corresponding to the halo formation criteria at a slightly higher redshift). The resulting new probability is a function of the environmental density and the descendant and progenitor halo masses. Its derivative with respect to the descendant and the progenitor masses yields the conditional halo mass function as a function of the overdensity of the larger-scale environment, which will be the main result of this paper. In §2, we provide a summary of the excursion set model and the path-integral approach to the non-Markovian extension. In §3, we introduce the formalism and perform the main calculation, including the simplification of the final result in the limit of the large scale environment.

2. NON-MARKOVIAN EXTENSION TO THE EXCURSION SET MODEL

2.1. Summary of the excursion set model

At any given time t and position \mathbf{x} , a virialized dark matter halo is formed in the excursion set model if the linear mass overdensity $\delta(\mathbf{x}, R)$ smoothed on the scale of the halo size R exceeds a threshold δ_c that is determined by the spherical collapse model, and if no larger smoothing scales meet the criterion. The smoothed density field is given by

$$\delta(\mathbf{x}, R) = \int d^3x' W(|\mathbf{x} - \mathbf{x}'|, R) \delta(\mathbf{x}'), \quad (1)$$

where $\delta(\mathbf{x}) = \rho(\mathbf{x})/\bar{\rho} - 1$ is the density contrast about the mean mass density $\bar{\rho}$ of the universe, $W(|\mathbf{x} - \mathbf{x}'|, R)$ is the smoothing filter function, and R is the smoothing scale. When W is a tophat function in k -space, the overdensity traces out the smoothing scale as a Markovian random walk process. Instead of R , the variance S of the density field is often used to denote the length (or mass) scale, where

$$S(R) \equiv \sigma^2(R) = \int \frac{d^3k}{(2\pi)^3} P(k) \tilde{W}^2(k, R). \quad (2)$$

Here $P(k)$ is the power spectrum of the matter density fluctuations in a given cosmological model, and \tilde{W} is the Fourier transform of the filter function W . As the smoothing radius R goes to infinity, $S(R)$ goes to zero. In hierarchical models of structure formation such as the Λ CDM model, S is a monotonically decreasing function of R . The variables S , R , and the associated mass, $M = (4/3)\pi R^3 \bar{\rho}$, can therefore be used interchangeably.

In the standard excursion set model, the first crossing distribution of random walks with a constant barrier δ_c

determines the halo mass function. Further refinement is achieved by the ellipsoidal collapse model with a scale-dependent δ_c (Sheth et al 2001; Sheth & Tormen 2002), or a diffusing barrier (Robertson et al. 2009; Maggiore & Riotto 2010b). The resulting halo mass functions are found to agree reasonably well with N -body simulation results (e.g., Tinker et al. 2008; Ma et al. 2011).

In addition to the halo mass function, the excursion set model also predicts the halo assembly history. As the linear density field grows with time, halos are identified on increasingly larger mass scales, which signifies the gain of dark matter mass through mergers or accretion. Statistics such as the halo merger rates, progenitor mass functions, and their relations with the large scale environmental density can all be worked out in this framework.

The calculation of the halo statistics typically treats the change of the smoothed linear density field δ with a decreasing smoothing scale $S(R)$ as a Markovian process, in which each step of the random walk is uncorrelated with the previous one. The Markovian assumption therefore decouples the linear density fluctuations below and beyond the halo mass scale, causing the halo properties, such as its formation time and merger rate, to be independent of the density of the halo environment. This assumption greatly simplifies the calculations and has led to a number of useful analytic results. The Markovianity of the process, however, relies on the density smoothing filter being a tophat function in k -space, which does not correspond to a well-defined halo mass in real space. In addition, the decoupling between halo mass and halo environment is not seen in numerical simulations.

2.2. Introduce non-Markovianity

A difficulty of the excursion set model is that an unambiguous relation between the smoothing radius R and the mass M of the corresponding collapsed halo only exists when the filter is a tophat function in real space: $M(R) = (4/3)\pi R^3 \bar{\rho}$. For all other filter functions (e.g., tophat in k -space, Gaussian), it is impossible to associate a well-defined mass $M(R)$ (see, e.g., Bond et al. 1991; Zentner 2007).

To deal with this problem, Maggiore & Riotto (2010a) uses a path integral approach to compute the probability associated with each trajectory $\delta(S)$ and sum over all relevant trajectories. For convenience, the time variable is first discretized and the continuum limit is taken at the end. Specifically, we discretize the interval $[0, S]$ in steps $\Delta S = \epsilon$, so $S_k = k\epsilon$ with $k = 1, \dots, n$, and the end point is $S_n \equiv S$. A trajectory is defined by the collection of values $\{\delta_1, \dots, \delta_n\}$, such that $\delta(S_k) = \delta_k$. All trajectories start at a value δ_0 at “time” $S = 0$.

The basic quantity in this approach is the probability density in the space of trajectories, defined as

$$W(\delta_0; \delta_1, \dots, \delta_n; S_n) \equiv \langle \delta_D[\delta(S_1) - \delta_1] \dots \delta_D[\delta(S_n) - \delta_n] \rangle \quad (3)$$

where δ_D is the Dirac delta function, and all trajectories start from δ_0 at $S = 0$. For a Gaussian random density field, the only non-zero component in W is the connected two-point correlator $\langle \delta_j \delta_k \rangle_c$, and W can be transformed into:

$$W(\delta_0; \delta_1, \dots, \delta_n; S_n) = \int_{-\infty}^{\infty} \frac{d\lambda_1}{2\pi} \dots \frac{d\lambda_n}{2\pi} \quad (4)$$

$$\times \exp \left(i \sum_{j=1}^n \lambda_j \delta_j - \frac{1}{2} \sum_{j,k=1}^n \lambda_j \lambda_k \langle \delta_j \delta_k \rangle_c \right).$$

If the density smoothing filter is a top-hat function in k -space, the evolution of $\delta(S)$ is Markovian, and the density correlation is:

$$\langle \delta_i \delta_j \rangle_c = \min(S_i, S_j). \quad (5)$$

In this case, the integrals in equation (4) can be worked out directly to give

$$W^{gm}(\delta_0; \delta_1, \dots, \delta_n; S_n) \quad (6)$$

$$= \frac{1}{(2\pi\epsilon)^{n/2}} \exp \left[-\frac{1}{2\epsilon} \sum_{i=0}^{n-1} (\delta_{i+1} - \delta_i)^2 \right],$$

where the superscript ‘‘gm’’ refers to the ‘‘Gaussian and Markovian’’ case. When the density smoothing filter is *not* a top-hat function in k -space, e.g., a top-hat function in real space or a Gaussian function, MR10 showed that an additional term appeared in the density correlation:

$$\langle \delta_i \delta_j \rangle_c = \min(S_i, S_j) + \Delta(S_i, S_j), \quad (7)$$

where $\Delta(S_i, S_j)$ is well approximated by

$$\Delta(S_i, S_j) \approx \kappa \frac{S_{\min}(S_{\max} - S_{\min})}{S_{\max}}, \quad (8)$$

$$S_{\max} = \max(S_i, S_j), \quad S_{\min} = \min(S_i, S_j).$$

The parameter κ characterizes the non-Markovian process, whose value depends on the shape of the smoothing filter, e.g., $\kappa \simeq 0.44$ for a top-hat function in real space, and $\kappa \approx 0.35$ for a Gaussian function.

For convenience, we use Δ_{ij} to denote $\Delta(S_i, S_j)$ in this paper. In the non-Markovian case, equation (4) can be expanded perturbatively into

$$W(\delta_0; \delta_1, \dots, \delta_n; S_n) \quad (9)$$

$$\approx \left(1 + \frac{1}{2} \sum_{i,j=1}^n \Delta_{ij} \frac{\partial^2}{\partial \delta_i \partial \delta_j} \right) W^{gm}(\delta_0; \delta_1, \dots, \delta_n; S_n).$$

We will use equation (9) for the rest of paper, keeping in mind that this relation only includes the leading order non-Markovian corrections.

3. MAIN DERIVATION

3.1. Introduce the environmental variable

The new ingredient that we will introduce into the non-Markovian excursion set model is the linear overdensity, δ_e , that quantifies the larger-scale environment of a dark matter halo. We denote the smoothing scale over which δ_e is evaluated as S_e , where S is defined in equation (2).

Throughout the paper, we use subscripts ‘‘e’’, ‘‘d’’, and ‘‘p’’ to denote environment, descendant, and progenitor, respectively. We consider a descendant halo of mass M_d , or $S_d = S(M_d)$, that formed at redshift z_d when the barrier height is $\delta_{cd} = \delta_c/D(z_d)$, where $\delta_c = 1.68$ and $D(z)$ is the linear growth function. We consider the probability for the descendant halo to have a progenitor halo of mass M_p , or $S_p = S(M_p)$, that formed at a higher redshift z_p when the barrier height is higher: $\delta_{cp} = \delta_c/D(z_p)$. We adopt the convention that the critical overdensity,

instead of the linear overdensity, is a function of redshift. The linear overdensity is always evaluated at redshift zero, including that on the environmental scale.

As an initial setup, we define three events A, B, and C as follows.

A: At a location of interest, the overdensity smoothed over a scale S_e (centered on the location) is δ_e .

B: At the same location as in A, a halo of mass S_d forms at redshift z_d , corresponding to barrier $\delta_{cd} = \delta_c/D(z_d)$, where $S_d > S_e$.

C: At the same location as in A, a progenitor halo of mass S_p forms at redshift z_p , corresponding to barrier $\delta_{cp} = \delta_c/D(z_p)$, where $z_p > z_d$ and $S_p > S_d > S_e$.

We then define the following probabilities that relate the three events above:

1. $P(A)d\delta_e$ is the probability that the linear overdensity smoothed over scale S_e is between δ_e and $\delta_e + d\delta_e$. For a Gaussian field, we have the simple relation

$$P(A) = \exp(-\delta_e^2/2S_e)/\sqrt{2\pi S_e}. \quad (10)$$

2. $P(A, B)d\delta_e dS_d$ is the probability that a halo of mass between S_d and $S_d + dS_d$ forms at redshift z_d , and at the halo location, the linear overdensity smoothed over a larger scale S_e is between δ_e and $\delta_e + d\delta_e$. More explicitly, we have

$$P(A, B) = P_{AB}(S_d, z_d, S_e, \delta_e). \quad (11)$$

3. $P(A, B, C)d\delta_e dS_d dS_p$ is the probability that a halo of mass between S_d and $S_d + dS_d$ forms at redshift z_d , and the mass of this halo at an earlier redshift z_p is in progenitor of mass between S_p and $S_p + dS_p$, and at the halo location, the linear overdensity on scale of S_e is between δ_e and $\delta_e + d\delta_e$. More explicitly, we have

$$P(A, B, C) = P_{ABC}(S_p, z_p, S_d, z_d, S_e, \delta_e). \quad (12)$$

Our goal is to derive expressions for the following conditional probabilities that depend on the halo environment parameterized by δ_e and S_e :

1. $P(B|A)dS_d$ is the probability that a halo of mass between S_d and $S_d + dS_d$ forms at redshift z_d in an environment of linear overdensity δ_e on scale of S_e . More explicitly, we have

$$P(B|A) = P_{(B|A)}(S_d, z_d | S_e, \delta_e). \quad (13)$$

As we show in Sec. 3.2, this quantity is simply related to the environment-dependent halo mass function.

2. For a halo of mass S_d forming at redshift z_d , located in the center of an environment of scale S_e and linear overdensity δ_e , $P(C|A, B)dS_p$ is the probability that the mass of this halo at an earlier redshift z_p is in progenitor of mass between S_p and $S_p + dS_p$. More explicitly, we have

$$P(C|A, B) = P_{(C|A, B)}(S_p, z_p | S_d, z_d, S_e, \delta_e). \quad (14)$$

As we show in Sec. 3.2, this quantity is simply related to the environment-dependent progenitor mass function

and the halo merger rate.

The probabilities are related by $P(B|A) = P(A, B)/P(A)$, $P(C|A, B) = P(A, B, C)/P(A, B)$. When the smoothing filter is chosen to be a top-hat function in k -space, the random walk is a Markovian process. The environmental dependence drops out in this case, and we have $P(C|A, B) = P(C|B)$, which is related to the standard progenitor mass function.

3.2. Relate probability functions to halo mass functions and merger rates

We define $n(M_d, z_d|S_e, \delta_e)dM_d$ as the mean number density of (descendant) halos of mass between M_d and $M_d + dM_d$ at redshift z_d residing in a region of linear overdensity δ_e smoothed over scale S_e . This halo mass function is simply related to the conditional probability $P(B|A)$ (denoted as $P_{(B|A)}$ below) by

$$n(M_d, z_d|S_e, \delta_e) = \frac{\bar{\rho}}{M_d} \left| \frac{dS_d}{dM_d} \right| P_{(B|A)}(S_d, z_d|S_e, \delta_e), \quad (15)$$

where $\bar{\rho}$ is the mean mass density.

Similarly, we define $N(M_p, z_p|M_d, z_d, S_e, \delta_e)dM_p$ as the mean number of progenitor halos of mass between M_p and $M_p + dM_p$ at redshift z_p for a descendant halo of mass M_d and redshift z_d residing in an environment of scale S_e and linear overdensity δ_e . This progenitor mass function is simply related to the conditional probability $P(C|A, B)$ (denoted as $P_{(C|A, B)}$ below) by

$$\begin{aligned} N(M_p, z_p|M_d, z_d, S_e, \delta_e) & \quad (16) \\ &= \frac{M_d}{M_p} \left| \frac{dS_p}{dM_p} \right| P_{(C|A, B)}(S_p, z_p|S_d, z_d, S_e, \delta_e). \end{aligned}$$

The halo merger rate can be written in terms of the progenitor mass function above. To this end, we adopt the binary merger assumption as in Zhang et al. (2008), and define $R(M, \xi, z|S_e, \delta_e)$ (same as the B/n term in equation (8) of Fakhouri & Ma 2009) to be the number of mergers per unit progenitor mass ratio ξ (ratio of the small to the large progenitor mass) and unit redshift for each descendant halo of mass M at redshift z , under the condition that the linear overdensity on the environmental scale S_e is δ_e . Due to the binary merger assumption, the merger rate R can be related to the progenitor mass function via¹

$$\begin{aligned} R(M_d, \xi, z_d|S_e, \delta_e) & \quad (17) \\ &= \frac{M_d}{(1 + \xi)^2} \frac{d}{dz} N \left(\frac{M_d \xi}{1 + \xi}, z|M_d, z_d, S_e, \delta_e \right) \Big|_{z=z_d}. \end{aligned}$$

Equations (15)-(17) enable us to obtain the environment-dependent halo mass functions and halo merger rates from $P(B|A)$ and $P(C|A, B)$. Since $P(B|A) = P(A, B)/P(A)$ and $P(C|A, B) =$

¹ Note that it is also possible to use $R(M, \xi, z|S_e, \delta_e) = M(1 + \xi)^{-2} dN(M/(1 + \xi), z|M, z, S_e, \delta_e)/dz|_{z'=z}$ to relate the merger rate to the progenitor mass function. In the limit of small Δz , these two relations should be equivalent. However, it has been found that this is generally not true in theories based the excursion set. In this paper, we simply use equation (17), which is found to work better in terms of comparison with simulation results in Zhang et al. (2008).

$P(A, B, C)/P(A, B)$, our next task is therefore to calculate $P(A, B)$ and $P(A, B, C)$.

3.3. Express $P(A, B)$ in path integral form

According to the definition of $P(A, B)$ in §3.1, we have

$$\begin{aligned} \int_{S_d}^{\infty} dS'_d P_{AB}(S'_d, z_d, S_e, \delta_e) &= \int_{-\infty}^{\delta_{cd}} d\delta_1 \dots \widehat{d\delta_m} \dots d\delta_n \\ &\times W(0; \delta_1, \dots, \delta_m = \delta_e, \dots, \delta_n; S_d), \end{aligned} \quad (18)$$

where the positions of S_e and S_d are approximated as $m\epsilon$ and $n\epsilon$, respectively, with m and n being integers. In other words, $S_m = S_e$, $S_n = S_d$ and $\delta_m = \delta_e$. The hat over $d\delta_m$ means that $d\delta_m$ is omitted from the list of integration variables.

By taking partial derivatives with respect to S_d on both sides of equation (18), and using equation (9), we obtain

$$\begin{aligned} P(A, B) &= P_{AB}(S_d, z_d, \delta_e, S_e) \quad (19) \\ &= -\frac{\partial}{\partial S_d} \int_{-\infty}^{\delta_{cd}} d\delta_1 \dots \widehat{d\delta_m} \dots d\delta_n \left(1 + \frac{1}{2} \sum_{i, j=1}^n \Delta_{ij} \partial_i \partial_j \right) \\ &\times W^{gm}(0; \delta_1, \dots, \delta_m = \delta_e, \dots, \delta_n; S_d). \end{aligned}$$

The terms proportional to Δ_{ij} are the non-Markovian corrections.

We rewrite the summation in the non-Markovian terms in equation (19) as

$$\frac{1}{2} \sum_{i, j=1}^n \Delta_{ij} \partial_i \partial_j = \sum_{i=1}^{n-1} \Delta_{in} \partial_i \partial_n + \sum_{i < j < n} \Delta_{ij} \partial_i \partial_j, \quad (20)$$

where $\Delta_{ii} = 0$ for $i = 1, 2, \dots, n$ based on equation (8) and is therefore not included. It can be shown that the first term on the right-hand side of equation (20) is zero. The second term can be broken into five pieces, representing all the possible locations of i and j with respect to m and n :

$$\begin{aligned} \sum_{i < j < n} &= \sum_{j=m+1}^{n-1} \cdot \sum_{i=m+1}^{j-1} + \sum_{j=m+1}^{n-1} \cdot (i = m) \quad (21) \\ &+ \sum_{j=m+1}^{n-1} \cdot \sum_{i=1}^{m-1} + (j = m) \cdot \sum_{i=1}^{m-1} + \sum_{j=1}^{m-1} \cdot \sum_{i=1}^{j-1}. \end{aligned}$$

In total, $P(A, B)$ in equation (19) is the sum of the Markovian term and the five terms in equation (21). We write these six terms as

$$P(A, B) = P_{AB}^M + P_{AB}^{NM1} + \dots + P_{AB}^{NM5}. \quad (22)$$

The superscripts M and NM refer to Markovian and Non-Markovian, respectively, and the number following each NM refers to the order of the term on the right-hand side of equation (21).

The algebra involved in deriving these six terms is straightforward but lengthy. We leave the details to Appendix A. The final expression for $P(A, B)$ is given by equation (38).

3.4. Express $P(A, B, C)$ in path integral form

The derivation of $P(A, B, C)$ is similar to that of $P(A, B)$ above but is more complicated. According to the definition of $P(A, B, C)$ in §3.1, we have

$$\begin{aligned} & \left(\int_{S_d}^{S_p} dS'_d \int_{S_p}^{\infty} dS'_p + \int_{S_p}^{\infty} dS'_d \int_{S'_d}^{\infty} dS'_p \right) \quad (23) \\ & \times P_{ABC}(S'_p, z_p, S'_d, z_d, S_e, \delta_e) \\ & = \int_{-\infty}^{\delta_{cd}} d\delta_1 \dots \widehat{d\delta_m} \dots d\delta_n \int_{-\infty}^{\delta_{cp}} d\delta_{n+1} \dots d\delta_N \\ & \times W(0; \delta_1, \dots, \delta_m = \delta_e, \dots, \delta_N; S_p), \end{aligned}$$

where the positions of S_e , S_d , and S_p are approximated as $m\epsilon$, $n\epsilon$, and $N\epsilon$, respectively, with m , n , and N being integers. In other words, $S_m = S_e$, $S_n = S_d$, $S_N = S_p$, and $\delta_m = \delta_e$. The hat over $d\delta_m$ means that $d\delta_m$ is omitted from the list of integration variables.

By taking partial derivatives with respect to both S_p and S_d on the two sides of equation (23), and using equation (9), we obtain

$$\begin{aligned} P(A, B, C) &= P_{ABC}(S_p, z_p, S_d, z_d, S_e, \delta_e) \quad (24) \\ &= \frac{\partial^2}{\partial S_d \partial S_p} \int_{-\infty}^{\delta_{cd}} d\delta_1 \dots \widehat{d\delta_m} \dots d\delta_n \int_{-\infty}^{\delta_{cp}} d\delta_{n+1} \dots d\delta_N \\ & \left(1 + \frac{1}{2} \sum_{i,j=1}^N \Delta_{ij} \partial_i \partial_j \right) W^{gm}(0; \delta_1, \dots, \delta_m = \delta_e, \dots, \delta_N; S_p). \end{aligned}$$

The terms proportional to Δ_{ij} are the non-Markovian corrections.

Similar to equation (20), we rewrite the summation in the non-Markovian terms above as

$$\frac{1}{2} \sum_{i,j=1}^N \Delta_{ij} \partial_i \partial_j = \sum_{i=1}^{N-1} \Delta_{iN} \partial_i \partial_N + \sum_{i < j < N} \Delta_{ij} \partial_i \partial_j. \quad (25)$$

As before, the first term here is always zero. We decompose the rest into thirteen terms:

$$\begin{aligned} \sum_{i < j < N} &= \sum_{j=n+1}^{N-1} \cdot \sum_{i=1}^{m-1} + \sum_{j=n+1}^{N-1} \cdot (i=m) \quad (26) \\ &+ \sum_{j=n+1}^{N-1} \cdot \sum_{i=m+1}^{n-1} + \sum_{j=n+1}^{N-1} \cdot (i=n) \\ &+ \sum_{j=n+1}^{N-1} \cdot \sum_{i=n+1}^{j-1} + (j=n) \cdot \sum_{i=1}^{m-1} \\ &+ (j=n) \cdot (i=m) + (j=n) \cdot \sum_{i=m+1}^{n-1} \\ &+ \sum_{j=m+1}^{n-1} \cdot \sum_{i=1}^{m-1} + \sum_{j=m+1}^{n-1} \cdot (i=m) \\ &+ \sum_{j=m+1}^{n-1} \cdot \sum_{i=m+1}^{j-1} + (j=m) \cdot \sum_{i=1}^{m-1} + \sum_{j=1}^{m-1} \cdot \sum_{i=1}^{j-1}. \end{aligned}$$

Again, we denote the Markovian part of $P(A, B, C)$ as P_{ABC}^M , and the thirteen non-Markovian terms on

the right-hand side of equation (26) as P_{ABC}^{NM1} , ..., and P_{ABC}^{NM13} . The probability $P(A, B, C)$ is then

$$P(A, B, C) = P_{ABC}^M + P_{ABC}^{NM1} + \dots + P_{ABC}^{NM13}. \quad (27)$$

We leave the details of the derivation of these fourteen terms to Appendix B. The final expression for $P(A, B, C)$ is given by equation (44).

3.5. Asymptotic forms in the limit of large environmental scale

As shown in § 3.3, 3.4, and Appendix A and B, the general forms of $P(A, B)$, $P(A, B, C)$, and $P(C|A, B)$ contain many terms. In practice, it is often unnecessary to consider the general case. Here, we derive the simplified forms of $P(B|A)$ and $P(C|A, B)$ in the limit of large environmental scale, which is usually the case considered in simulations and observations. We leave the details of the derivation to Appendix C and quote the final results here.

To linear order in δ_e , the probability of forming a descendant halo of mass $S_d = S(M_d)$ at redshift z_d that resides in a larger environment of overdensity δ_e smoothed over scale S_e is

$$\begin{aligned} P(B|A) &= P_{(B|A)}(S_d, z_d | S_e, \delta_e) \quad (28) \\ &\approx \frac{\delta_{cd}}{\sqrt{2\pi} S_d^{3/2}} \exp\left(-\frac{\nu^2}{2}\right) \\ &\times \left\{ 1 - \kappa + \frac{\kappa}{2} \exp\left(\frac{\nu^2}{2}\right) \Gamma\left(0, \frac{\nu^2}{2}\right) \right. \\ &\left. + \frac{\delta_e}{\delta_{cd}} \left[\nu^2 - 1 + \kappa - \frac{\kappa}{2} \exp\left(\frac{\nu^2}{2}\right) \Gamma\left(0, \frac{\nu^2}{2}\right) \right] \right\}, \end{aligned}$$

where $\nu \equiv \delta_{cd}/\sqrt{S_d}$, $\delta_{cd} = \delta_c/D(z_d)$ is the barrier height for forming a descendant halo at redshift z_d , $\Gamma(0, x)$ is the incomplete Gamma function, and κ is the non-Markovian parameter defined in equation (8). We note that this equation is identical to equation (24) of Ma et al. (2011) for the conditional first crossing rate, which was used to derive the halo bias parameter. In the limit of $\delta_e \rightarrow 0$, we recover from equation (28) the non-Markovian extension of the standard halo mass function (see, e.g., Table 1 of Ma et al. 2011):

$$\begin{aligned} P(B) &= \frac{\delta_{cd}}{\sqrt{2\pi} S_d^{3/2}} \exp\left(-\frac{\nu^2}{2}\right) \quad (29) \\ &\times \left[1 - \kappa + \frac{\kappa}{2} \exp\left(\frac{\nu^2}{2}\right) \Gamma\left(0, \frac{\nu^2}{2}\right) \right]. \end{aligned}$$

Similarly, the conditional probability (to linear order in δ_e) that a descendant halo of mass $S_d = S(M_d)$ at redshift z_d , residing in a larger environment of overdensity δ_e at scale S_e , has a progenitor halo of mass $S_p = S(M_p)$ at redshift z_p (assuming $z_p \approx z_d$) is

$$\begin{aligned} P(C|A, B) &= P_{(C|A, B)}(S_p, z_p | S_d, z_d, S_e, \delta_e) \quad (30) \\ &\approx \frac{\delta_{cp} - \delta_{cd}}{\sqrt{2\pi}(S_p - S_d)^{3/2}} \left\{ 1 + \kappa\beta\alpha - \sqrt{2\pi}\kappa\nu(1 - \alpha)^{3/2} \right. \\ &\left. + \pi\kappa \left(\nu^2 \frac{\delta_e}{\delta_{cd}} - 1 \right) (1 - \alpha)^{3/2} \exp\left[\frac{\nu^2}{2}\right] \operatorname{erfc}\left[\frac{\nu}{\sqrt{2}}\right] \right\}, \end{aligned}$$

where $\alpha \equiv S_d/S_p$, and β is a simple algebraic function of α

$$\beta = -2 + \frac{(1-\alpha)^{3/2}}{2\alpha} \ln \left(\frac{1 + \sqrt{1-\alpha}}{1 - \sqrt{1-\alpha}} \right) + \frac{1}{\alpha} + 2\alpha. \quad (31)$$

The variables $\delta_{cp} = \delta_c/D(z_p)$ and $\delta_{cd} = \delta_c/D(z_d)$ specify the barrier heights for forming the progenitor and descendant halos at redshift z_p and z_d , respectively. Equations (10) and (11) relate $P(C|A,B)$ above to the mean progenitor mass function $N(M_p, z_p|M_d, z_d, S_e, \delta_e)$ and the merger rate $R(M_d, \xi, z|S_e, \delta_e)$. In the Markovian limit ($\kappa = 0$), we note that equation (30) reduces to the familiar conditional mass function of small look-back time ($\delta_{cp} - \delta_{cd}$) predicted by the excursion set model, and the dependence on the environmental overdensity δ_e drops out. This limit confirms that the introduction of the non-Markovian process to the excursion set model is the key in introducing the environmental dependence of halo formation history.

Finally, the accuracy of the simple spherical collapse model can be improved by considering a diffusing barrier instead of a constant one. The introduction of the diffusing barrier is motivated by both the elliptical collapse model and N -body studies, for the reason that realistic halos are triaxial rather than spherical. For our purpose, we only need to replace δ_c by $\delta_c/\sqrt{1+D_B}$ and κ by $\kappa/(1+D_B)$ in our formulae to take into account the diffusing barrier effect (Robertson et al. 2009; Maggiore & Riotto 2010b), with $D_B = 0.25$.

3.6. Numerical results

In Figure 1, we illustrate the numerical results from our analytic formulae for the halo mass function $n(M_d, z_d|S_e, \delta_e)$ (upper panels) and the merger rate $R(M_d, \xi, z_d|S_e, \delta_e)$ (lower panels) as a function of the halo environment δ_e . Three descendant halo masses at $z_d = 0$ are shown for comparison: $M_d = 10^{11}$ (blue), 10^{12} (green), $10^{13} M_\odot$ (red). The environmental mass scale S_e is chosen to be $10^{17} M_\odot$. The full expressions (solid curves) are computed from equations (38) and (44), and the approximate expression (dotted curves), valid to linear order in δ_e , are computed from equations (28) and (30). The diffusing barrier effect is included in the right two panels with $D_B = 0.25$, and not included in the left two panels (*i.e.*, $D_B = 0$). The cosmological model is a Λ CDM model with $\Omega_m = 0.25$, $\Omega_b = 0.045$, $\Omega_\Lambda = 0.75$, $h = 0.73$, and an initial power-law power spectrum of the density fluctuation with index $n = 1$, and normalization $\sigma_8 = 0.9$.

The lower panels of Figure 1 shows a positive dependence of the merger rate on δ_e . Since equations (16) and (17) indicate that the progenitor mass function has the same dependence on δ_e as the halo merger rate, our results imply that progenitor mass functions are also higher in regions with higher δ_e . This environmental trend is consistent with that seen for halo merger rates in the Millennium simulation (Fakhouri & Ma 2008, 2009, 2010), where the amplitudes of the merger rate and progenitor mass functions increase with the environmental overdensities. The black solid curves in the lower panels of Figure 1 show the environmental dependence from the second formula in equation (11) of Fakhouri & Ma (2009). The larger-scale overdensity in this case is δ_7 and is mea-

sured within a comoving radius of $R = 7h^{-1} \text{Mpc}$ centered at each halo in the simulation. As Figure 1 shows, the overall dependence of the merger rate on δ_e is similar, while the slope of the curves from our analytic model has a weak dependence on halo mass. As discussed in detail in Fakhouri & Ma (2009), there are various options for quantifying halo environment in simulations. For instance, the environmental overdensity can be computed by either including or excluding the virial mass of the central halo within the sphere of radius R over which δ_e is computed. For simplicity, equation (11) of Fakhouri & Ma (2009) provides two separate fits for δ_7 and $\delta_{7\text{-FOF}}$, where the latter excludes the halo's FOF mass. They also noted that the difference between the two definitions, $\delta_7 - \delta_{7\text{-FOF}}$, is a function of halo mass, increasing from ~ 0.01 at $10^{12} M_\odot$ to ~ 10 at $10^{15} M_\odot$. Given this uncertainty and mass dependence, it is therefore not surprising that our analytic model predicts mass-dependent slopes in Figure 1. A closer comparison between our model prediction and simulation results would require a more elaborate mapping between the linear δ_e in the excursion set model and the nonlinear δ_7 and $\delta_{7\text{-FOF}}$ used in the simulation. We leave this step to future studies.

4. SUMMARY

We have presented a method to introduce ‘‘assembly bias’’ into the excursion set model for the formation and growth of dark matter halos. Our calculation is based on the barrier-crossing problem of non-Markovian processes, which we solve perturbatively using the path integral formalism developed in MR10. The new variable that we introduced to parameterize a halo's larger-scale environment is the linear overdensity field δ_e smoothed over a chosen scale of S_e , where S_e is the variance of the linear density fluctuations and is a monotonically decreasing function of the smoothing radius R .

To introduce environmental dependence, we isolated δ_e from the path integral over the probability density of trajectories W in equation (18). We then derived the two main probability functions $P(A, B)$ and $P(A, B, C)$, defined in Sec 3.1, for forming descendant and progenitor halos *in an environment* in which the linear overdensity smoothed over scale S_e is given by δ_e . The calculations are set up in Sec. 3.3 and 3.4, and the details of how to manipulate the numerous integrals are given in Appendix A and B. The final analytic expressions for $P(A, B)$ and $P(A, B, C)$ are given by equations (38) and (44), respectively.

The three key physical quantities that we investigated in this paper are the descendant halo mass function $n(M_d, z_d|S_e, \delta_e)$, the progenitor mass function $N(M_p, z_p|M_d, z_d, S_e, \delta_e)$, and the halo merger rate $R(M_d, \xi, z_d|S_e, \delta_e)$. These quantities are related to the conditional probabilities $P(B|A)$ and $P(C|A, B)$ by equations (15)-(17), which in turn can be computed from our formulae for $P(A, B)$ and $P(A, B, C)$.

Since the full expressions for the mass functions and merger rates are complicated, we derived their asymptotic forms in the limit of large environmental scale (*i.e.*, small S_e and δ_e) in §3.5 and Appendix C. This is a useful limit for many practical purposes. The approximate expressions for the descendant mass function and progenitor mass function are given by equations (28) and (30), respectively. Figure 1 illustrates the environmental de-

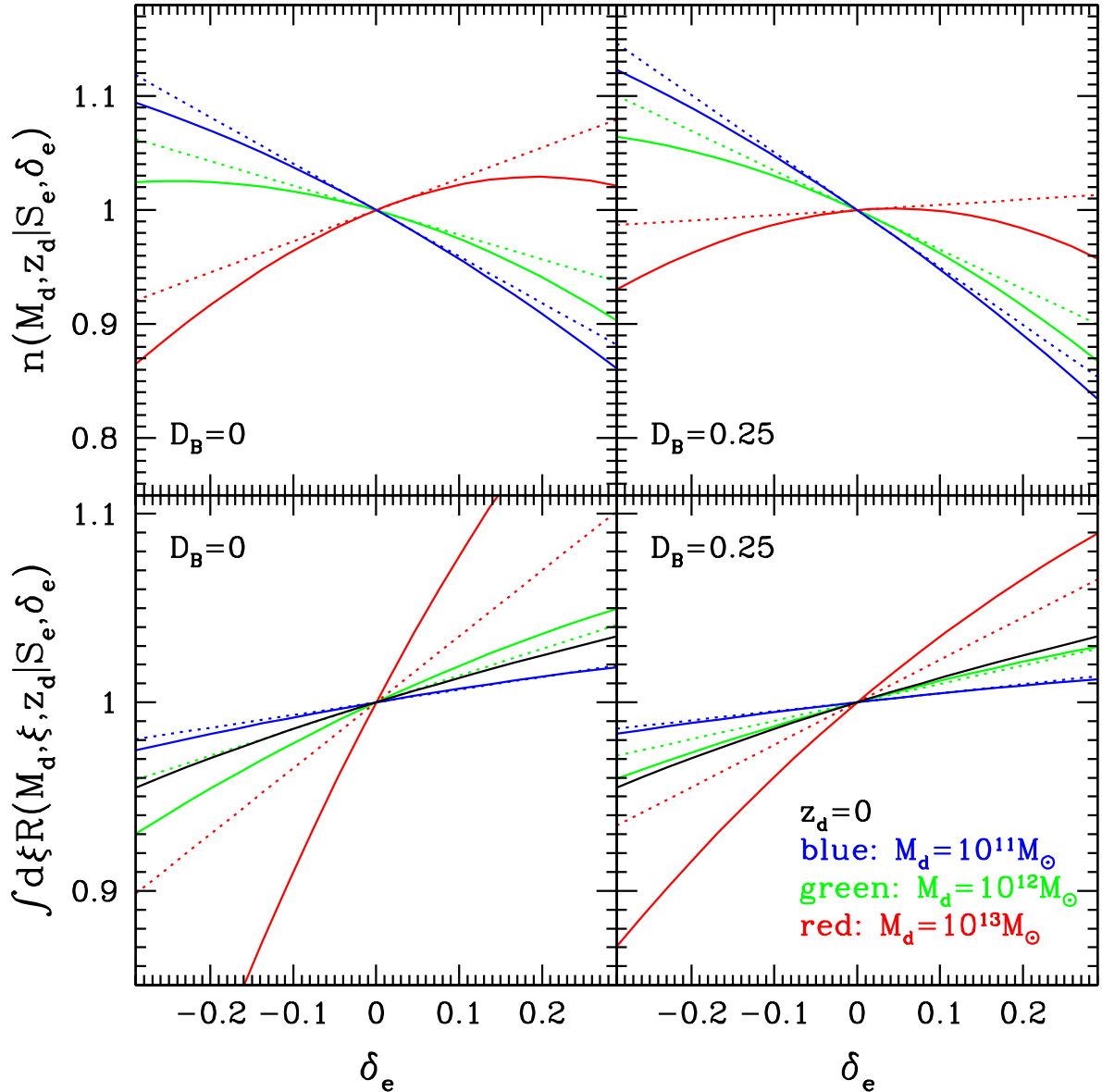


FIG. 1.— Environmental dependence of the halo mass function $n(M_d, z_d | S_e, \delta_e)$ (upper panels) and the halo merger rate $R(M_d, \xi, z_d | S_e, \delta_e)$ for merger mass ratio above 0.01 (i.e. $\xi = 0.01$ to 1) (lower panels). Two types of barriers in the excursion set model are shown for comparison: constant $\delta_c = 1.68$ (left panels) and the diffusing barrier $\delta_c/\sqrt{1+D_B}$ with $D_B = 0.25$ (right panels). In each panel, the results are shown for three descendant halo masses: $M_d = 10^{11}$ (blue), 10^{12} (green), $10^{13} M_\odot$ (red) at redshift $z_d = 0$, and the environmental mass scale is $S_e = 10^{17} M_\odot$. The vertical axis in each panel is normalized to the value when the environmental overdensity field δ_e is zero. The full expressions from equations (38) and (44) are shown as colored solid curves; the approximate expressions (valid to linear order in δ_e) from equations (28) and (30) are shown as colored dotted curves. As equations (16) and (17) indicate, the progenitor mass function has the same dependence on δ_e as that in the lower panels. The black solid curves in the lower panels plot the merger rates from equation (11) of Fakhouri & Ma (2009), which is obtained from the Millennium simulation.

pendence predicted by our model. It is encouraging that both our analytic calculation and N -body results show that the halo merger rate and progenitor mass function correlate positively with the environmental density.

The recipe presented in this paper for incorporating environmental dependence into the excursion set model is quite general. It should provide a useful theoretical framework for future investigations into how the spatial distributions and statistical properties of dark matter halos depend on their mass as well as their assembly history and the larger-scale environment in which they reside.

JZ is supported by the National Science Foundation of China under grant No. 11273018, the National Basic Research Program of China (2013CB834900), the national Thousand Talents Program for distinguished young scholars, a grant (No.11DZ2260700) from the Office of Science and Technology in Shanghai Municipal Government, and the T.D. Lee Scholarship from the Center for High Energy Physics of Peking University. JZ was previously supported by the TCC Fellowship of UT Austin and the TAC Fellowship of UC Berkeley, where a part of this work was done. Support for CPM is provided in part by grants from the Simons Foundation (#224959), NASA NNX11A197G, and HST-AR-

12140.01-A from the Space Telescope Science Institute. AR is supported by the Swiss National Science Foun-

ation (SNSF), project ‘‘The non-Gaussian Universe’’ (project number: 200021140236).

REFERENCES

- Angulo, R. E., Baugh, C. M., & Lacey, C. G. 2008, MNRAS, 387, 921
 Avila-Reese V., Colin P., Gottlöber S., Firmani C., Maulbetsch C., 2005, ApJ, 634, 51
 Bett P., Eke V., Frenk C. S., Jenkins A., Helly J., Navarro J., 2007, MNRAS, 376, 215
 Bond J., Cole S., Efstathiou G., Kaiser N., 1991, ApJ, 379, 440.
 Dalal N., White M., Bond J. R., Shirokov A., 2008, ApJ, 687, 12
 Desjacques V., 2008, MNRAS, 388, 638
 Fakhouri O., Ma C.-P., 2008, MNRAS, 386, 577
 Fakhouri O., Ma C.-P., 2009, MNRAS, 394, 1825
 Fakhouri O., Ma C.-P., 2010, MNRAS, 401, 2245
 Faltenbacher, A., White S. D. M., 2010, ApJ, 708, 469
 Gao L., Springel V., White S. D. M., 2005, MNRAS, 363, L66
 Gao L., White S. D. M., 2007, MNRAS, 377, L5
 Gottlöber S., Klypin A., Kravtsov A. V., 2001, ApJ, 546, 223
 Harker G., Cole S., Helly J., Frenk C., Jenkins A., 2006, MNRAS, 367, 1039
 Jing Y. P., Suto Y., Mo H. J., 2007, ApJ, 657, 664
 Lacey C. & Cole S., 1993, MNRAS, 262, 627L
 Li Y., Mo H. J., Gao L., 2008, MNRAS, 389, 1419
 Ma C.-P., Maggiore, M., Riotto, A., & Zhang, J. 2011, MNRAS, 411, 2644
 Maggiore, M. & Riotto, A., 2010(a), ApJ, 711, 907.
 Maggiore, M. & Riotto, A., 2010(b), ApJ, 717, 515
 Maulbetsch C., Avila-Reese V., Colin P., Gottlöber S., Khalatyan A., Steinmetz M., 2007, ApJ, 654, 53
 Press W. H. & Schechter P., 1974, ApJ, 187, 425.
 Robertson, B., Kravtsov, A., Tinker, J., Zentner, A., 2009, ApJ, 696, 636
 Sandvik H. B., Moller O., Lee J., White S. D. M., 2007, MNRAS, 377, 234
 Sheth R., Mo H., Tormen G., 2001, MNRAS, 323, 1
 Sheth R. & Tormen G., 2002, MNRAS, 329, 61
 Sheth R. & Tormen G., 2004, MNRAS, 350, 1385
 Tinker J., Kravtsov A. V., Klypin A., Abazajian K., Warren M., Yepes G., Gottlöber S., Holz D. E., 2008, ApJ, 688, 709
 Wang H. Y., Mo H. J., Jing Y. P., 2007, MNRAS, 375, 633
 Wechsler R. H., Zentner A. R., Bullock J. S., Kravtsov A. V., Allgood B., 2006, ApJ, 652, 71
 Wetzel, A. R., Cohn, J. D., White, M., Holz, D. E., & Warren, M. S. 2007, ApJ, 656, 139
 Zentner A., 2007, Int. J. Mod. Phys. D, 16, 763.
 Zentner A., Hearin A., & van den Bosch F., 2013, arXiv: 1311.1818
 Zhang J., Ma C.-P., & Fakhouri O., 2008, MNRAS, 387, L13

APPENDIX A – DERIVATION OF $P(A, B)$

In this appendix, we carry out the integral in equation (19) explicitly and derive an expression for each of the six terms in the summation in equation (22). We begin with the following relations from MR10:

$$\begin{aligned} W^{gm}(\delta_0; \delta_1, \dots, \delta_n; S_n) &= W^{gm}(\delta_0; \delta_1, \dots, \delta_i; S_i) W^{gm}(\delta_i; \delta_{i+1}, \dots, \delta_n; S_n - S_i), \\ \Pi_\epsilon^{\delta_c}(\delta_0; \delta_n; S_n) &\equiv \int_{-\infty}^{\delta_c} d\delta_1 \dots \int_{-\infty}^{\delta_c} d\delta_{n-1} W^{gm}(\delta_0; \delta_1, \dots, \delta_n; S_n). \end{aligned} \quad (32)$$

For the Markovian term in $P(A, B)$ of equation (22), we find

$$P_{AB}^M = -\frac{\partial}{\partial S_n} \int_{-\infty}^{\delta_{cd}} d\delta_n \Pi_\epsilon^{\delta_{cd}}(0; \delta_e; S_m) \Pi_\epsilon^{\delta_{cd}}(\delta_e; \delta_n; S_n - S_m). \quad (33)$$

For the five non-Markovian terms, we find

$$\begin{aligned} P_{AB}^{NM1} &= -\sum_{j=m+1}^{n-1} \sum_{i=m+1}^{j-1} \Delta_{ij} \frac{\partial}{\partial S_n} \int_{-\infty}^{\delta_{cd}} d\delta_n \Pi_\epsilon^{\delta_{cd}}(0; \delta_e; S_m) \Pi_\epsilon^{\delta_{cd}}(\delta_e; \delta_{cd}; S_i - S_m) \\ &\quad \times \Pi_\epsilon^{\delta_{cd}}(\delta_{cd}; \delta_{cd}; S_j - S_i) \Pi_\epsilon^{\delta_{cd}}(\delta_{cd}; \delta_n; S_n - S_j), \\ P_{AB}^{NM2} &= -\sum_{j=m+1}^{n-1} \Delta_{mj} \frac{\partial^2}{\partial \delta_e \partial S_n} \int_{-\infty}^{\delta_{cd}} d\delta_n \Pi_\epsilon^{\delta_{cd}}(0; \delta_e; S_m) \Pi_\epsilon^{\delta_{cd}}(\delta_e; \delta_{cd}; S_j - S_m) \Pi_\epsilon^{\delta_{cd}}(\delta_{cd}; \delta_n; S_n - S_j), \\ P_{AB}^{NM3} &= -\sum_{j=m+1}^{n-1} \sum_{i=1}^{m-1} \Delta_{ij} \frac{\partial}{\partial S_n} \int_{-\infty}^{\delta_{cd}} d\delta_n \Pi_\epsilon^{\delta_{cd}}(0; \delta_{cd}; S_i) \Pi_\epsilon^{\delta_{cd}}(\delta_{cd}; \delta_e; S_m - S_i) \\ &\quad \times \Pi_\epsilon^{\delta_{cd}}(\delta_e; \delta_{cd}; S_j - S_m) \Pi_\epsilon^{\delta_{cd}}(\delta_{cd}; \delta_n; S_n - S_j), \\ P_{AB}^{NM4} &= -\sum_{i=1}^{m-1} \Delta_{im} \frac{\partial^2}{\partial \delta_e \partial S_n} \int_{-\infty}^{\delta_{cd}} d\delta_n \Pi_\epsilon^{\delta_{cd}}(0; \delta_{cd}; S_i) \Pi_\epsilon^{\delta_{cd}}(\delta_{cd}; \delta_e; S_m - S_i) \Pi_\epsilon^{\delta_{cd}}(\delta_e; \delta_n; S_n - S_m), \\ P_{AB}^{NM5} &= -\sum_{j=1}^{m-1} \sum_{i=1}^{j-1} \Delta_{ij} \frac{\partial}{\partial S_n} \int_{-\infty}^{\delta_{cd}} d\delta_n \Pi_\epsilon^{\delta_{cd}}(0; \delta_{cd}; S_i) \Pi_\epsilon^{\delta_{cd}}(\delta_{cd}; \delta_{cd}; S_j - S_i) \\ &\quad \times \Pi_\epsilon^{\delta_{cd}}(\delta_{cd}; \delta_e; S_m - S_j) \Pi_\epsilon^{\delta_{cd}}(\delta_e; \delta_n; S_n - S_m). \end{aligned} \quad (34)$$

To transform the summations into integrations and further simplify these expressions, we use the following relations from MR10:

$$\begin{aligned}\Pi_{\epsilon \rightarrow 0}^{\delta_c}(\delta_0; \delta; S)(\delta_0, \delta \neq \delta_c) &= \frac{1}{\sqrt{2\pi S}} \left[e^{-(\delta - \delta_0)^2/(2S)} - e^{-(2\delta_c - \delta_0 - \delta)^2/(2S)} \right], \quad \Pi_{\epsilon \rightarrow 0}^{\delta_c}(\delta_c; \delta_c; S) = \frac{\epsilon}{\sqrt{2\pi S^{3/2}}}, \quad (35) \\ \Pi_{\epsilon \rightarrow 0}^{\delta_c}(\delta_0; \delta_c; S)(\delta_0 \neq \delta_c) &= \sqrt{\frac{\epsilon}{\pi}} \frac{\delta_c - \delta_0}{S^{3/2}} e^{-(\delta_c - \delta_0)^2/(2S)}, \quad \Pi_{\epsilon \rightarrow 0}^{\delta_c}(\delta_c; \delta; S)(\delta \neq \delta_c) = \sqrt{\frac{\epsilon}{\pi}} \frac{\delta_c - \delta}{S^{3/2}} e^{-(\delta_c - \delta)^2/(2S)}.\end{aligned}$$

Substituting these expressions into equations (33) and (34), we obtain

$$P_{AB}^M = -\Pi_0^{\delta_{cd}}(0; \delta_e; S_m) \frac{\partial}{\partial S_n} \int_{-\infty}^{\delta_{cd}} d\delta_n \Pi_0^{\delta_{cd}}(\delta_e; \delta_n; S_n - S_m), \quad (36)$$

$$\begin{aligned}P_{AB}^{NM1} &= -\frac{1}{\pi\sqrt{2\pi}} \Pi_0^{\delta_{cd}}(0; \delta_e; S_m) \frac{\partial}{\partial S_n} \int_{-\infty}^{\delta_{cd}} d\delta_n \int_{S_m}^{S_n} dS_j \int_{S_m}^{S_j} dS_i \Delta(S_i, S_j) \\ &\quad \times \frac{1}{(S_j - S_i)^{3/2}} \frac{\delta_{cd} - \delta_e}{(S_i - S_m)^{3/2}} \frac{\delta_{cd} - \delta_n}{(S_n - S_j)^{3/2}} \exp \left[-\frac{(\delta_{cd} - \delta_e)^2}{2(S_i - S_m)} - \frac{(\delta_{cd} - \delta_n)^2}{2(S_n - S_j)} \right], \quad (37) \\ P_{AB}^{NM2} &= -\frac{1}{\pi} \frac{\partial^2}{\partial \delta_e \partial S_n} \Pi_0^{\delta_{cd}}(0; \delta_e; S_m) \int_{-\infty}^{\delta_{cd}} d\delta_n \int_{S_m}^{S_n} dS_j \Delta(S_m, S_j) \\ &\quad \times \frac{\delta_{cd} - \delta_e}{(S_j - S_m)^{3/2}} \frac{\delta_{cd} - \delta_n}{(S_n - S_j)^{3/2}} \exp \left[-\frac{(\delta_{cd} - \delta_e)^2}{2(S_j - S_m)} - \frac{(\delta_{cd} - \delta_n)^2}{2(S_n - S_j)} \right], \\ P_{AB}^{NM3} &= -\frac{1}{\pi^2} \frac{\partial}{\partial S_n} \int_{-\infty}^{\delta_{cd}} d\delta_n \int_{S_m}^{S_n} dS_j \int_0^{S_m} dS_i \Delta(S_i, S_j) \frac{\delta_{cd}}{S_i^{3/2}} \frac{\delta_{cd} - \delta_e}{(S_m - S_i)^{3/2}} \frac{\delta_{cd} - \delta_e}{(S_j - S_m)^{3/2}} \\ &\quad \times \frac{\delta_{cd} - \delta_n}{(S_n - S_j)^{3/2}} \exp \left[-\frac{\delta_{cd}^2}{2S_i} \right] \exp \left[-\frac{(\delta_{cd} - \delta_e)^2}{2(S_m - S_i)} - \frac{(\delta_{cd} - \delta_e)^2}{2(S_j - S_m)} - \frac{(\delta_{cd} - \delta_n)^2}{2(S_n - S_j)} \right], \\ P_{AB}^{NM4} &= -\frac{1}{\pi} \frac{\partial}{\partial \delta_e} \left[\frac{\partial}{\partial S_n} \int_{-\infty}^{\delta_{cd}} d\delta_n \Pi_0^{\delta_{cd}}(\delta_e; \delta_n; S_n - S_m) \right] \\ &\quad \times \int_0^{S_m} dS_i \Delta(S_i, S_m) \frac{\delta_{cd}}{S_i^{3/2}} \frac{\delta_{cd} - \delta_e}{(S_m - S_i)^{3/2}} \exp \left[-\frac{\delta_{cd}^2}{2S_i} - \frac{(\delta_{cd} - \delta_e)^2}{2(S_m - S_i)} \right], \\ P_{AB}^{NM5} &= -\frac{1}{\pi\sqrt{2\pi}} \left[\frac{\partial}{\partial S_n} \int_{-\infty}^{\delta_{cd}} d\delta_n \Pi_0^{\delta_{cd}}(\delta_e; \delta_n; S_n - S_m) \right] \\ &\quad \times \int_0^{S_m} dS_j \int_0^{S_j} dS_i \Delta(S_i, S_j) \frac{\delta_{cd}}{S_i^{3/2}} \frac{\delta_{cd} - \delta_e}{(S_j - S_i)^{3/2}} \frac{1}{(S_m - S_j)^{3/2}} \exp \left[-\frac{\delta_{cd}^2}{2S_i} - \frac{(\delta_{cd} - \delta_e)^2}{2(S_m - S_j)} \right].\end{aligned}$$

Using equation (7) for $\Delta(S_i, S_j)$, we can work out the integrals above. This step is straightforward but tedious, so we only present the final results here. We also replace S_m and S_n with the more physical notation for the environment and descendant: $S_m = S_e$ and $S_n = S_d$. Our final expression for $P(A, B)$ is given by

$$\begin{aligned}P(A, B) &= P_{AB}^M + P_{AB}^{NM1} + \dots + P_{AB}^{NM5} \quad (38) \\ &= \frac{1}{\sqrt{2\pi}} \frac{\delta_{cd} - \delta_e}{(S_d - S_e)^{3/2}} \left[1 + \kappa \frac{S_e}{S_d} \left(1 - \frac{(\delta_{cd} - \delta_e)^2}{S_d - S_e} \right) + \kappa \frac{\delta_e(\delta_{cd} - \delta_e)}{S_d} \right] \mathbf{E}_1 \mathbf{\Pi} \\ &\quad + \frac{\kappa}{2\sqrt{2\pi}} (\delta_{cd} - \delta_e) S_d^{-3/2} \mathbf{E}_2 \mathbf{\Pi} \mathbf{F}_1 + \frac{\kappa}{\pi} \delta_{cd} (\delta_{cd} - \delta_e)^2 S_e^{-3/2} (S_d - S_e)^{-3/2} \mathbf{E}_1 \mathbf{E}_3 \\ &\quad - \frac{\kappa}{2} \delta_{cd} (\delta_{cd} - \delta_e) S_e^{-1/2} S_d^{-3/2} \mathbf{E}_2 \mathbf{E} \mathbf{r}_2 \mathbf{\Pi} - \frac{\kappa}{2} \delta_{cd} (\delta_{cd} - \delta_e)^2 S_e^{-3/2} S_d^{-3/2} \mathbf{E}_2 \mathbf{E} \mathbf{r}_1 \mathbf{E} \mathbf{r}_2 \\ &\quad + \frac{\kappa}{\sqrt{2\pi}} \delta_{cd} (\delta_{cd} - \delta_e)^3 S_e^{-1} S_d^{-1} (S_d - S_e)^{-3/2} \mathbf{E}_1 \mathbf{E} \mathbf{r}_1 + \frac{\kappa}{\pi} \delta_{cd} (\delta_{cd} - \delta_e)^2 S_e^{-3/2} (S_d - S_e)^{-3/2} \mathbf{E}_1 \mathbf{F}_2,\end{aligned}$$

where

$$\begin{aligned}\mathbf{E}_1 &= \exp \left[-\frac{(\delta_{cd} - \delta_e)^2}{2(S_d - S_e)} \right], \quad \mathbf{E}_2 = \exp \left[\frac{(\delta_{cd} - \delta_e)^2}{2S_e} \right], \quad \mathbf{E}_3 = \exp \left[-\frac{(2\delta_{cd} - \delta_e)^2}{2S_e} \right], \quad (39) \\ \mathbf{E} \mathbf{r}_1 &= \operatorname{erfc} \left[\frac{2\delta_{cd} - \delta_e}{\sqrt{2S_e}} \right], \quad \mathbf{E} \mathbf{r}_2 = \operatorname{erfc} \left[\sqrt{\frac{S_d}{2(S_d - S_e)S_e}} (\delta_{cd} - \delta_e) \right], \quad \mathbf{E} \mathbf{r}_3 = \operatorname{erfc} \left[\frac{\delta_{cd} - \delta_e}{\sqrt{2(S_d - S_e)}} \right],\end{aligned}$$

$$\begin{aligned}\mathbf{\Pi} &= \Pi_0^{\delta_{cd}}(0; \delta_e; S_e), \quad \mathbf{F}[a(>0), b] = \int_a^{+\infty} \frac{dx}{x} e^{-(x+b)^2}, \\ \mathbf{F}_1 &= \mathbf{F} \left[\left(\sqrt{\frac{S_d}{S_d - S_e}} - 1 \right) \frac{\delta_{cd} - \delta_e}{\sqrt{2S_e}}, \frac{\delta_{cd} - \delta_e}{\sqrt{2S_e}} \right] - \mathbf{F} \left[\left(\sqrt{\frac{S_d}{S_d - S_e}} + 1 \right) \frac{\delta_{cd} - \delta_e}{\sqrt{2S_e}}, -\frac{\delta_{cd} - \delta_e}{\sqrt{2S_e}} \right], \\ \mathbf{F}_2 &= \mathbf{F} \left[\frac{\delta_{cd}}{\sqrt{2S_e}}, \frac{\delta_{cd} - \delta_e}{\sqrt{2S_e}} \right].\end{aligned}$$

APPENDIX B – DERIVATION OF $P(A, B, C)$

In this appendix, we carry out the integral in equation (24) explicitly and derive an expression for each of the fourteen terms in the summation in equation (27). For $P(A, B, C)$ in equation (27), we find the Markovian term to be

$$P_{ABC}^M = \frac{\partial^2}{\partial S_n \partial S_N} \int_{-\infty}^{\delta_{cd}} d\delta_n \int_{-\infty}^{\delta_{cp}} d\delta_N \Pi_\epsilon^{\delta_{cd}}(0; \delta_e; S_m) \Pi_\epsilon^{\delta_{cd}}(\delta_e; \delta_n; S_n - S_m) \Pi_\epsilon^{\delta_{cp}}(\delta_n; \delta_N; S_N - S_n), \quad (40)$$

and the thirteen non-Markovian terms to be

$$\begin{aligned}P_{ABC}^{NM1} &= \sum_{j=n+1}^{N-1} \sum_{i=1}^{m-1} \Delta_{ij} \frac{\partial^2}{\partial S_n \partial S_N} \int_{-\infty}^{\delta_{cd}} d\delta_n \int_{-\infty}^{\delta_{cp}} d\delta_N \Pi_\epsilon^{\delta_{cd}}(0; \delta_{cd}; S_i) \Pi_\epsilon^{\delta_{cd}}(\delta_{cd}; \delta_e; S_m - S_i) \\ &\quad \times \Pi_\epsilon^{\delta_{cd}}(\delta_e; \delta_n; S_n - S_m) \Pi_\epsilon^{\delta_{cp}}(\delta_n; \delta_{cp}; S_j - S_n) \Pi_\epsilon^{\delta_{cp}}(\delta_{cp}; \delta_N; S_N - S_j), \\ P_{ABC}^{NM2} &= \sum_{j=n+1}^{N-1} \Delta_{mj} \frac{\partial^3}{\partial \delta_e \partial S_n \partial S_N} \int_{-\infty}^{\delta_{cd}} d\delta_n \int_{-\infty}^{\delta_{cp}} d\delta_N \Pi_\epsilon^{\delta_{cd}}(0; \delta_e; S_m) \Pi_\epsilon^{\delta_{cd}}(\delta_e; \delta_n; S_n - S_m) \\ &\quad \times \Pi_\epsilon^{\delta_{cp}}(\delta_n; \delta_{cp}; S_j - S_n) \Pi_\epsilon^{\delta_{cp}}(\delta_{cp}; \delta_N; S_N - S_j), \\ P_{ABC}^{NM3} &= \sum_{j=n+1}^{N-1} \sum_{i=m+1}^{n-1} \Delta_{ij} \frac{\partial^2}{\partial S_n \partial S_N} \int_{-\infty}^{\delta_{cd}} d\delta_n \int_{-\infty}^{\delta_{cp}} d\delta_N \Pi_\epsilon^{\delta_{cd}}(0; \delta_e; S_m) \Pi_\epsilon^{\delta_{cd}}(\delta_e; \delta_{cd}; S_i - S_m) \\ &\quad \times \Pi_\epsilon^{\delta_{cd}}(\delta_{cd}; \delta_n; S_n - S_i) \Pi_\epsilon^{\delta_{cp}}(\delta_n; \delta_{cp}; S_j - S_n) \Pi_\epsilon^{\delta_{cp}}(\delta_{cp}; \delta_N; S_N - S_j), \\ P_{ABC}^{NM4} &= \sum_{j=n+1}^{N-1} \Delta_{nj} \frac{\partial^2}{\partial S_n \partial S_N} \int_{-\infty}^{\delta_{cp}} d\delta_N \Pi_\epsilon^{\delta_{cd}}(0; \delta_e; S_m) \Pi_\epsilon^{\delta_{cd}}(\delta_e; \delta_{cd}; S_n - S_m) \\ &\quad \times \Pi_\epsilon^{\delta_{cp}}(\delta_{cd}; \delta_{cp}; S_j - S_n) \Pi_\epsilon^{\delta_{cp}}(\delta_{cp}; \delta_N; S_N - S_j), \\ P_{ABC}^{NM5} &= \sum_{j=n+1}^{N-1} \sum_{i=n+1}^{j-1} \Delta_{ij} \frac{\partial^2}{\partial S_n \partial S_N} \int_{-\infty}^{\delta_{cd}} d\delta_n \int_{-\infty}^{\delta_{cp}} d\delta_N \Pi_\epsilon^{\delta_{cd}}(0; \delta_e; S_m) \Pi_\epsilon^{\delta_{cd}}(\delta_e; \delta_n; S_n - S_m) \\ &\quad \times \Pi_\epsilon^{\delta_{cp}}(\delta_n; \delta_{cp}; S_i - S_n) \Pi_\epsilon^{\delta_{cp}}(\delta_{cp}; \delta_{cp}; S_j - S_i) \Pi_\epsilon^{\delta_{cp}}(\delta_{cp}; \delta_N; S_N - S_j), \\ P_{ABC}^{NM6} &= \sum_{i=1}^{m-1} \Delta_{in} \frac{\partial^2}{\partial S_n \partial S_N} \int_{-\infty}^{\delta_{cp}} d\delta_N \Pi_\epsilon^{\delta_{cd}}(0; \delta_{cd}; S_i) \Pi_\epsilon^{\delta_{cd}}(\delta_{cd}; \delta_e; S_m - S_i) \Pi_\epsilon^{\delta_{cd}}(\delta_e; \delta_{cd}; S_n - S_m) \\ &\quad \times \Pi_\epsilon^{\delta_{cp}}(\delta_{cd}; \delta_N; S_N - S_n), \\ P_{ABC}^{NM7} &= \Delta_{mn} \frac{\partial^3}{\partial \delta_e \partial S_n \partial S_N} \int_{-\infty}^{\delta_{cp}} d\delta_N \Pi_\epsilon^{\delta_{cd}}(0; \delta_e; S_m) \Pi_\epsilon^{\delta_{cd}}(\delta_e; \delta_{cd}; S_n - S_m) \Pi_\epsilon^{\delta_{cp}}(\delta_{cd}; \delta_N; S_N - S_n), \\ P_{ABC}^{NM8} &= \sum_{i=m+1}^{n-1} \Delta_{in} \frac{\partial^2}{\partial S_n \partial S_N} \int_{-\infty}^{\delta_{cp}} d\delta_N \Pi_\epsilon^{\delta_{cd}}(0; \delta_e; S_m) \Pi_\epsilon^{\delta_{cd}}(\delta_e; \delta_{cd}; S_i - S_m) \Pi_\epsilon^{\delta_{cd}}(\delta_{cd}; \delta_{cd}; S_n - S_i) \\ &\quad \times \Pi_\epsilon^{\delta_{cp}}(\delta_{cd}; \delta_N; S_N - S_n), \\ P_{ABC}^{NM9} &= \sum_{j=m+1}^{n-1} \sum_{i=1}^{m-1} \Delta_{ij} \frac{\partial^2}{\partial S_n \partial S_N} \int_{-\infty}^{\delta_{cd}} d\delta_n \int_{-\infty}^{\delta_{cp}} d\delta_N \Pi_\epsilon^{\delta_{cd}}(0; \delta_{cd}; S_i) \Pi_\epsilon^{\delta_{cd}}(\delta_{cd}; \delta_e; S_m - S_i) \\ &\quad \times \Pi_\epsilon^{\delta_{cd}}(\delta_e; \delta_{cd}; S_j - S_m) \Pi_\epsilon^{\delta_{cd}}(\delta_{cd}; \delta_n; S_n - S_j) \Pi_\epsilon^{\delta_{cp}}(\delta_n; \delta_N; S_N - S_n), \\ P_{ABC}^{NM10} &= \sum_{j=m+1}^{n-1} \Delta_{mj} \frac{\partial^3}{\partial \delta_e \partial S_n \partial S_N} \int_{-\infty}^{\delta_{cd}} d\delta_n \int_{-\infty}^{\delta_{cp}} d\delta_N \Pi_\epsilon^{\delta_{cd}}(0; \delta_e; S_m) \Pi_\epsilon^{\delta_{cd}}(\delta_e; \delta_{cd}; S_j - S_m)\end{aligned}$$

$$\begin{aligned}
& \times \Pi_{\epsilon}^{\delta_{cd}}(\delta_{cd}; \delta_n; S_n - S_j) \Pi_{\epsilon}^{\delta_{cp}}(\delta_n; \delta_N; S_N - S_n), \\
P_{ABC}^{NM11} &= \sum_{j=m+1}^{n-1} \sum_{i=m+1}^{j-1} \Delta_{ij} \frac{\partial^2}{\partial S_n \partial S_N} \int_{-\infty}^{\delta_{cd}} d\delta_n \int_{-\infty}^{\delta_{cp}} d\delta_N \Pi_{\epsilon}^{\delta_{cd}}(0; \delta_e; S_m) \Pi_{\epsilon}^{\delta_{cd}}(\delta_e; \delta_{cd}; S_i - S_m) \\
& \times \Pi_{\epsilon}^{\delta_{cd}}(\delta_{cd}; \delta_{cd}; S_j - S_i) \Pi_{\epsilon}^{\delta_{cd}}(\delta_{cd}; \delta_n; S_n - S_j) \Pi_{\epsilon}^{\delta_{cp}}(\delta_n; \delta_N; S_N - S_n), \\
P_{ABC}^{NM12} &= \sum_{i=1}^{m-1} \Delta_{im} \frac{\partial^3}{\partial \delta_e \partial S_n \partial S_N} \int_{-\infty}^{\delta_{cd}} d\delta_n \int_{-\infty}^{\delta_{cp}} d\delta_N \Pi_{\epsilon}^{\delta_{cd}}(0; \delta_{cd}; S_i) \Pi_{\epsilon}^{\delta_{cd}}(\delta_{cd}; \delta_e; S_m - S_i) \\
& \times \Pi_{\epsilon}^{\delta_{cd}}(\delta_e; \delta_n; S_n - S_m) \Pi_{\epsilon}^{\delta_{cp}}(\delta_n; \delta_N; S_N - S_n), \\
P_{ABC}^{NM13} &= \sum_{j=1}^{m-1} \sum_{i=1}^{j-1} \Delta_{ij} \frac{\partial^2}{\partial S_n \partial S_N} \int_{-\infty}^{\delta_{cd}} d\delta_n \int_{-\infty}^{\delta_{cp}} d\delta_N \Pi_{\epsilon}^{\delta_{cd}}(0; \delta_{cd}; S_i) \Pi_{\epsilon}^{\delta_{cd}}(\delta_{cd}; \delta_{cd}; S_j - S_i) \\
& \times \Pi_{\epsilon}^{\delta_{cd}}(\delta_{cd}; \delta_e; S_m - S_j) \Pi_{\epsilon}^{\delta_{cd}}(\delta_e; \delta_n; S_n - S_m) \Pi_{\epsilon}^{\delta_{cp}}(\delta_n; \delta_N; S_N - S_n).
\end{aligned}$$

The fourteen expressions above can again be written out as

$$P_{ABC}^M = \Pi_0^{\delta_{cd}}(0; \delta_e; S_m) \frac{\partial^2}{\partial S_n \partial S_N} \int_{-\infty}^{\delta_{cd}} d\delta_n \int_{-\infty}^{\delta_{cp}} d\delta_N \Pi_0^{\delta_{cd}}(\delta_e; \delta_n; S_n - S_m) \Pi_0^{\delta_{cp}}(\delta_n; \delta_N; S_N - S_n), \quad (42)$$

$$\begin{aligned}
P_{ABC}^{NM1} &= \frac{1}{\pi^2} \frac{\partial^2}{\partial S_n \partial S_N} \int_{-\infty}^{\delta_{cd}} d\delta_n \int_{-\infty}^{\delta_{cp}} d\delta_N \Pi_0^{\delta_{cd}}(\delta_e; \delta_n; S_n - S_m) \int_0^{S_m} dS_i \int_{S_n}^{S_N} dS_j \Delta(S_i, S_j) \\
& \times \frac{\delta_{cd}}{S_i^{3/2}} \frac{\delta_{cd} - \delta_e}{(S_m - S_i)^{3/2}} \frac{\delta_{cp} - \delta_n}{(S_j - S_n)^{3/2}} \frac{\delta_{cp} - \delta_N}{(S_N - S_j)^{3/2}} \exp \left[-\frac{\delta_{cd}^2}{2S_i} - \frac{(\delta_{cd} - \delta_e)^2}{2(S_m - S_i)} - \frac{(\delta_{cp} - \delta_n)^2}{2(S_j - S_n)} - \frac{(\delta_{cp} - \delta_N)^2}{2(S_N - S_j)} \right], \quad (43)
\end{aligned}$$

$$\begin{aligned}
P_{ABC}^{NM2} &= \frac{1}{\pi} \frac{\partial^3}{\partial \delta_e \partial S_n \partial S_N} \int_{-\infty}^{\delta_{cd}} d\delta_n \int_{-\infty}^{\delta_{cp}} d\delta_N \Pi_0^{\delta_{cd}}(0; \delta_e; S_m) \Pi_0^{\delta_{cd}}(\delta_e; \delta_n; S_n - S_m) \\
& \times \int_{S_n}^{S_N} dS_j \Delta(S_m, S_j) \frac{\delta_{cp} - \delta_n}{(S_j - S_n)^{3/2}} \frac{\delta_{cp} - \delta_N}{(S_N - S_j)^{3/2}} \exp \left[-\frac{(\delta_{cp} - \delta_n)^2}{2(S_j - S_n)} - \frac{(\delta_{cp} - \delta_N)^2}{2(S_N - S_j)} \right],
\end{aligned}$$

$$\begin{aligned}
P_{ABC}^{NM3} &= \frac{1}{\pi^2} \Pi_0^{\delta_{cd}}(0; \delta_e; S_m) \frac{\partial^2}{\partial S_n \partial S_N} \int_{-\infty}^{\delta_{cd}} d\delta_n \int_{-\infty}^{\delta_{cp}} d\delta_N \int_{S_n}^{S_N} dS_j \int_{S_m}^{S_n} dS_i \Delta(S_i, S_j) \\
& \times \frac{\delta_{cd} - \delta_e}{(S_i - S_m)^{3/2}} \frac{\delta_{cd} - \delta_n}{(S_n - S_i)^{3/2}} \frac{\delta_{cp} - \delta_n}{(S_j - S_n)^{3/2}} \frac{\delta_{cp} - \delta_N}{(S_N - S_j)^{3/2}} \\
& \times \exp \left[-\frac{(\delta_{cd} - \delta_e)^2}{2(S_i - S_m)} - \frac{(\delta_{cd} - \delta_n)^2}{2(S_n - S_i)} - \frac{(\delta_{cp} - \delta_n)^2}{2(S_j - S_n)} - \frac{(\delta_{cp} - \delta_N)^2}{2(S_N - S_j)} \right],
\end{aligned}$$

$$P_{ABC}^{NM4} = 0,$$

$$\begin{aligned}
P_{ABC}^{NM5} &= \frac{1}{\pi \sqrt{2\pi}} \Pi_0^{\delta_{cd}}(0; \delta_e; S_m) \frac{\partial^2}{\partial S_n \partial S_N} \int_{-\infty}^{\delta_{cd}} d\delta_n \int_{-\infty}^{\delta_{cp}} d\delta_N \Pi_0^{\delta_{cd}}(\delta_e; \delta_n; S_n - S_m) \\
& \times \int_{S_n}^{S_N} dS_j \int_{S_n}^{S_j} dS_i \Delta(S_i, S_j) \frac{1}{(S_j - S_i)^{3/2}} \frac{\delta_{cp} - \delta_n}{(S_i - S_n)^{3/2}} \frac{\delta_{cp} - \delta_N}{(S_N - S_j)^{3/2}} \exp \left[-\frac{(\delta_{cp} - \delta_n)^2}{2(S_i - S_n)} - \frac{(\delta_{cp} - \delta_N)^2}{2(S_N - S_j)} \right],
\end{aligned}$$

$$P_{ABC}^{NM6} = P_{ABC}^{NM7} = P_{ABC}^{NM8} = 0,$$

$$\begin{aligned}
P_{ABC}^{NM9} &= \frac{1}{\pi^2} \frac{\partial^2}{\partial S_n \partial S_N} \int_{-\infty}^{\delta_{cd}} d\delta_n \int_{-\infty}^{\delta_{cp}} d\delta_N \Pi_0^{\delta_{cp}}(\delta_n; \delta_N; S_N - S_n) \int_{S_m}^{S_n} dS_j \int_0^{S_m} dS_i \Delta(S_i, S_j) \\
& \times \frac{\delta_{cd}}{S_i^{3/2}} \frac{\delta_{cd} - \delta_e}{(S_m - S_i)^{3/2}} \frac{\delta_{cd} - \delta_e}{(S_j - S_m)^{3/2}} \frac{\delta_{cd} - \delta_n}{(S_n - S_j)^{3/2}} \exp \left[-\frac{\delta_{cd}^2}{2S_i} - \frac{(\delta_{cd} - \delta_e)^2}{2(S_m - S_i)} - \frac{(\delta_{cd} - \delta_e)^2}{2(S_j - S_m)} - \frac{(\delta_{cd} - \delta_n)^2}{2(S_n - S_j)} \right],
\end{aligned}$$

$$\begin{aligned}
P_{ABC}^{NM10} &= \frac{1}{\pi} \frac{\partial^3}{\partial \delta_e \partial S_n \partial S_N} \int_{-\infty}^{\delta_{cd}} d\delta_n \int_{-\infty}^{\delta_{cp}} d\delta_N \Pi_0^{\delta_{cd}}(0; \delta_e; S_m) \Pi_0^{\delta_{cp}}(\delta_n; \delta_N; S_N - S_n) \\
& \times \int_{S_m}^{S_n} dS_j \Delta(S_m, S_j) \frac{\delta_{cd} - \delta_e}{(S_j - S_m)^{3/2}} \frac{\delta_{cd} - \delta_n}{(S_n - S_j)^{3/2}} \exp \left[-\frac{(\delta_{cd} - \delta_e)^2}{2(S_j - S_m)} - \frac{(\delta_{cd} - \delta_n)^2}{2(S_n - S_j)} \right],
\end{aligned}$$

$$P_{ABC}^{NM11} = \frac{1}{\pi \sqrt{2\pi}} \Pi_0^{\delta_{cd}}(0; \delta_e; S_m) \frac{\partial^2}{\partial S_n \partial S_N} \int_{-\infty}^{\delta_{cd}} d\delta_n \int_{-\infty}^{\delta_{cp}} d\delta_N \Pi_0^{\delta_{cp}}(\delta_n; \delta_N; S_N - S_n)$$

$$\begin{aligned}
& \times \int_{S_m}^{S_n} dS_j \int_{S_m}^{S_j} dS_i \Delta(S_i, S_j) \frac{1}{(S_j - S_i)^{3/2}} \frac{\delta_{cd} - \delta_e}{(S_i - S_m)^{3/2}} \frac{\delta_{cd} - \delta_n}{(S_n - S_j)^{3/2}} \exp \left[-\frac{(\delta_{cd} - \delta_e)^2}{2(S_i - S_m)} - \frac{(\delta_{cd} - \delta_n)^2}{2(S_n - S_j)} \right], \\
P_{ABC}^{NM12} &= \frac{1}{\pi} \frac{\partial^3}{\partial \delta_e \partial S_n \partial S_N} \int_{-\infty}^{\delta_{cd}} d\delta_n \int_{-\infty}^{\delta_{cp}} d\delta_N \Pi_0^{\delta_{cd}}(\delta_e; \delta_n; S_n - S_m) \Pi_0^{\delta_{cp}}(\delta_n; \delta_N; S_N - S_n) \\
& \times \int_0^{S_m} dS_i \Delta(S_i, S_m) \frac{\delta_{cd}}{S_i^{3/2}} \frac{\delta_{cd} - \delta_e}{(S_m - S_i)^{3/2}} \exp \left[-\frac{\delta_{cd}^2}{2S_i} - \frac{(\delta_{cd} - \delta_e)^2}{2(S_m - S_i)} \right], \\
P_{ABC}^{NM13} &= \frac{1}{\pi \sqrt{2\pi}} \frac{\partial^2}{\partial S_n \partial S_N} \int_{-\infty}^{\delta_{cd}} d\delta_n \int_{-\infty}^{\delta_{cp}} d\delta_N \Pi_0^{\delta_{cd}}(\delta_e; \delta_n; S_n - S_m) \Pi_0^{\delta_{cp}}(\delta_n; \delta_N; S_N - S_n) \\
& \times \int_0^{S_m} dS_j \int_0^{S_j} dS_i \Delta(S_i, S_j) \frac{1}{(S_j - S_i)^{3/2}} \frac{\delta_{cd}}{S_i^{3/2}} \frac{\delta_{cd} - \delta_e}{(S_m - S_j)^{3/2}} \exp \left[-\frac{\delta_{cd}^2}{2S_i} - \frac{(\delta_{cd} - \delta_e)^2}{2(S_m - S_j)} \right].
\end{aligned}$$

For simplicity, the calculation of P_{ABC} is done in the limit of $\delta_{cp} - \delta_{cd} \ll 1$. The lowest order term of the final result is proportional to $\delta_{cp} - \delta_{cd}$. This is because when $\delta_{cp} = \delta_{cd}$, the integrals in equation (24) is independent of the descendent halo mass S_d .

We now replace S_m, S_n , and S_N with the more physical notation for the environment, descendant, and progenitor: $S_m = S_e, S_n = S_d$, and $S_N = S_p$. Our final expression for $P(A, B, C)$ is

$$\begin{aligned}
P(A, B, C) &= P_{ABC}^M + P_{ABC}^{NM1} + \dots + P_{ABC}^{NM13} \\
&= \frac{\delta_{cp} - \delta_{cd}}{2\pi} (\delta_{cd} - \delta_e) (S_d - S_e)^{-3/2} (S_p - S_d)^{-3/2} \mathbf{E}_1 \mathbf{\Pi} \\
&+ \kappa (\delta_{cp} - \delta_{cd}) \left\{ -\frac{1}{2\sqrt{2\pi}} \delta_{cd} (\delta_{cd} - \delta_e)^2 S_d^{-3/2} S_p^{-3/2} (S_d - S_e)^{-3/2} \mathbf{E}_1 \mathbf{E}_1 \mathbf{E}_1 \right. \\
&+ \frac{1}{2\sqrt{2\pi}} S_e^2 S_d^{-3/2} S_p^{-3/2} (S_d - S_e)^{-3/2} \left[1 - \frac{\delta_e (\delta_{cd} - \delta_e)}{S_e} + \frac{(\delta_{cd} - \delta_e)^2}{S_d - S_e} \left(1 - \frac{2S_d^2}{S_e^2} \right) \right] \mathbf{E}_1 \mathbf{\Pi} \\
&+ \frac{1}{2\pi} (\delta_{cd} - \delta_e) (S_d - S_e)^{-3/2} (S_p - S_d)^{-3/2} \left[\frac{S_d}{S_p} \mathbf{G}_1 + \frac{\delta_e (\delta_{cd} - \delta_e)}{S_d} - \frac{(\delta_{cd} - \delta_e)^2 S_e}{S_d - S_e} \frac{1}{S_d} \right] \mathbf{E}_1 \mathbf{\Pi} \\
&+ \frac{1}{2\pi} \delta_{cd} (\delta_{cd} - \delta_e)^3 S_e^{-1} (S_d - S_e)^{-5/2} (S_p - S_e)^{-2} (S_p - S_d)^{-1/2} \mathbf{E}_1 \mathbf{E}_1 \mathbf{G}_2 \\
&- \frac{1}{2\sqrt{2\pi}} \delta_{cd} (\delta_{cd} - \delta_e)^2 S_e^{-3/2} S_d^{-3/2} (S_p - S_d)^{-3/2} \mathbf{E}_2 \mathbf{E}_1 \mathbf{E}_2 \\
&- \frac{1}{2\sqrt{2\pi}} \delta_{cd} (\delta_{cd} - \delta_e) S_e^{-1/2} S_d^{-3/2} (S_p - S_d)^{-3/2} \mathbf{E}_2 \mathbf{E}_2 \mathbf{\Pi} \\
&+ \frac{1}{4\pi} (\delta_{cd} - \delta_e) S_d^{-3/2} (S_p - S_d)^{-3/2} \mathbf{E}_2 \mathbf{\Pi} \mathbf{F}_1 - \frac{1}{2} (\delta_{cd} - \delta_e) S_d^{-3/2} S_p^{-3/2} \mathbf{E}_3 \mathbf{\Pi} \\
&+ \frac{1}{2\pi} (\delta_{cd} - \delta_e) S_e S_d^{-3/2} S_p^{-2} (S_d - S_e)^{-1} (S_p - S_d)^{-1/2} \left(S_d - \frac{1}{2} S_p \right) \mathbf{\Pi} \\
&\times \exp \left[-\frac{(\delta_{cd} - \delta_e)^2}{2S_e} \left(\frac{S_d}{S_d - S_e} + 2\sqrt{\frac{S_d}{S_d - S_e}} \right) \right] \\
&+ \left. \frac{1}{\pi \sqrt{2\pi}} \delta_{cd} (\delta_{cd} - \delta_e)^2 S_e^{-3/2} (S_d - S_e)^{-3/2} (S_p - S_d)^{-3/2} \mathbf{E}_1 (\mathbf{E}_3 + \mathbf{F}_2) \right\},
\end{aligned} \tag{44}$$

where

$$\begin{aligned}
\mathbf{G}_1 &= -1 + \frac{1}{2} S_d^{-1} S_p^{-1/2} (S_p - S_d)^{3/2} \ln \frac{\sqrt{S_p} + \sqrt{S_p - S_d}}{\sqrt{S_p} - \sqrt{S_p - S_d}} + S_p S_d^{-2} (S_d + S_e) \\
&+ S_d^{-2} S_p^{-1} \left(S_d - \frac{1}{2} S_p \right) [2S_d^2 + (S_d + S_e)(S_p - S_d)] - S_d^{-3/2} S_p^{-1} (S_d - S_e)^{1/2} (S_p - S_d) \left(S_d - \frac{1}{2} S_p \right)
\end{aligned} \tag{45}$$

and

$$\mathbf{G}_2 = 6S_d - 2S_e - 4S_p - (S_d - S_e)(S_p - S_d)^{-1} (S_p - S_e) + S_d^{-1} (2S_d - S_e)(S_p - S_e)^2 (S_p - S_d)^{-1}. \tag{46}$$

APPENDIX C – $P(A, B)$ AND $P(A, B, C)$ IN THE LIMIT OF LARGE ENVIRONMENTAL SCALE

In the limit of large environmental scale, i.e., small S_e , the overdensity smoothed over this scale, δ_e , also becomes a small parameter because $\langle \delta_e^2 \rangle \sim S_e$. We will therefore assume S_e is of the same order as δ_e^2 , while keeping in mind that δ_e^2/S_e is not necessarily small. The conditional probability $P(C|A, B)$ is equal to the ratio of $P(A, B, C)$ in equation (44) and $P(A, B)$ in equation (38), each of which contains special functions defined in equation (39). The key step in simplifying $P(C|A, B)$ is to find the behavior of these special functions in the limit of small S_e . After some algebra, we obtain

$$\begin{aligned} \mathbf{E}_1 &\approx \exp\left[-\frac{(\delta_{cd} - \delta_e)^2}{2S_d}\right], & \mathbf{\Pi} &\approx \frac{1}{\sqrt{2\pi S_e}} \exp\left[-\frac{\delta_e^2}{2S_e}\right], & \mathbf{Er}_1 &\approx \frac{\sqrt{2S_e}}{\sqrt{\pi}(2\delta_{cd} - \delta_e)} \exp\left[-\frac{(2\delta_{cd} - \delta_e)^2}{2S_e}\right], \\ \mathbf{Er}_2 &\approx \frac{\sqrt{2S_e}}{\sqrt{\pi}(\delta_{cd} - \delta_e)} \exp\left[-\frac{(\delta_{cd} - \delta_e)^2}{2S_e} - \frac{(\delta_{cd} - \delta_e)^2}{2S_d}\right], & \mathbf{Er}_3 &\approx \operatorname{erfc}\left[\frac{\delta_{cd} - \delta_e}{\sqrt{2S_d}}\right], \\ \mathbf{F}_1 &\approx \exp\left[-\frac{(\delta_{cd} - \delta_e)^2}{2S_e}\right] \Gamma\left[0, \frac{(\delta_{cd} - \delta_e)^2}{2S_d}\right], & \mathbf{F}_2 &\approx \frac{S_e}{\delta_{cd}(2\delta_{cd} - \delta_e)} \exp\left[-\frac{(2\delta_{cd} - \delta_e)^2}{2S_e}\right]. \end{aligned} \quad (47)$$

Note that \mathbf{E}_2 and \mathbf{E}_3 in equation (39) are not included here, because their forms cannot and need not be further simplified. The new forms of \mathbf{Er}_1 , \mathbf{Er}_2 , and \mathbf{Er}_3 are based on the formula

$$\lim_{a \rightarrow +\infty} \operatorname{erfc}[a] \rightarrow \frac{1}{a\sqrt{\pi}} \exp[-a^2], \quad (48)$$

which can be derived from

$$\begin{aligned} \lim_{a \rightarrow +\infty} \operatorname{erfc}[a] &= \lim_{a \rightarrow +\infty} \frac{2}{\sqrt{\pi}} \int_a^{+\infty} \exp(-x^2) dx \\ &= \lim_{a \rightarrow +\infty} \frac{2}{\sqrt{\pi}} \exp(-a^2) \int_a^{+\infty} \exp(a^2 - x^2) dx \\ &= \lim_{a \rightarrow +\infty} \frac{1}{\sqrt{\pi}} \exp(-a^2) \int_0^{+\infty} \frac{\exp(-t) dt}{\sqrt{t + a^2}} \quad [\text{Let : } t = x^2 - a^2] \\ &= \lim_{a \rightarrow +\infty} \frac{1}{a\sqrt{\pi}} \exp(-a^2) \int_0^{+\infty} \exp(-t) \left[1 + \mathcal{O}\left(\frac{t}{a^2}\right)\right] dt \\ &= \lim_{a \rightarrow +\infty} \frac{1}{a\sqrt{\pi}} \exp(-a^2) [1 + \mathcal{O}(a^{-2})] \\ &\rightarrow \frac{1}{a\sqrt{\pi}} \exp[-a^2]. \end{aligned} \quad (49)$$

The simplifications of \mathbf{F}_1 and \mathbf{F}_2 are similar. We need to use the relations

$$\lim_{a, b \rightarrow +\infty} \mathbf{F}(a, b) \rightarrow \frac{1}{2a(a+b)} \exp[-(a+b)^2], \quad \lim_{b \rightarrow +\infty, ab \rightarrow c(>0)} [\mathbf{F}(a, b) - \mathbf{F}(a+2b, -b)] \rightarrow \exp[-b^2] \Gamma(0, 2c). \quad (50)$$

Equation (50) can be worked out as follows:

$$\begin{aligned} &\lim_{a, b \rightarrow +\infty} \mathbf{F}[a, b] \\ &= \lim_{a, b \rightarrow +\infty} \int_a^{+\infty} \exp[-(x+b)^2] \frac{dx}{x} \\ &= \lim_{a, b \rightarrow +\infty} \exp[-(a+b)^2] \int_a^{+\infty} \exp[(a+b)^2 - (x+b)^2] \frac{dx}{x} \\ &= \lim_{a, b \rightarrow +\infty} \frac{1}{2} \exp[-(a+b)^2] \int_0^{+\infty} \frac{\exp(-t) dt}{\sqrt{t+(a+b)^2} [\sqrt{t+(a+b)^2} - b]} \quad [\text{Let : } t = (x+b)^2 - (a+b)^2] \\ &= \lim_{a, b \rightarrow +\infty} \frac{1}{2a(a+b)} \exp[-(a+b)^2] \int_0^{+\infty} \left\{1 + \mathcal{O}\left[\frac{t}{(a+b)^2}\right] + \mathcal{O}\left[\frac{t}{a(a+b)}\right]\right\} \exp(-t) dt \\ &\rightarrow \frac{1}{2a(a+b)} \exp[-(a+b)^2], \end{aligned} \quad (51)$$

$$\lim_{b \rightarrow +\infty, ab \rightarrow c(>0)} [\mathbf{F}(a, b) - \mathbf{F}(a+2b, -b)] \quad (52)$$

$$\begin{aligned}
&= \lim_{b \rightarrow +\infty, ab \rightarrow c(>0)} \int_a^{+\infty} \frac{dx}{x} \exp[-(x+b)^2] - \int_{a+2b}^{+\infty} \frac{dx}{x} \exp[-(x-b)^2] \\
&= \lim_{b \rightarrow +\infty, ab \rightarrow c(>0)} \int_{a+b}^{+\infty} \frac{dx}{x-b} \exp(-x^2) - \int_{a+b}^{+\infty} \frac{dx}{x+b} \exp(-x^2) \\
&= \lim_{b \rightarrow +\infty, ab \rightarrow c(>0)} \int_{a+b}^{+\infty} \frac{2b}{x^2 - b^2} \exp(-x^2) dx \\
&= \lim_{b \rightarrow +\infty, ab \rightarrow c(>0)} \exp[-(a+b)^2] \int_{a+b}^{+\infty} \frac{2b}{x^2 - b^2} \exp[(a+b)^2 - x^2] dx \\
&= \lim_{b \rightarrow +\infty, ab \rightarrow c(>0)} \exp[-(a+b)^2] b \int_0^{+\infty} \frac{\exp(-t) dt}{\sqrt{t + (a+b)^2} [t + (a+b)^2 - b^2]} \quad [\text{Let: } t = x^2 - (a+b)^2] \\
&= \lim_{b \rightarrow +\infty, ab \rightarrow c(>0)} \exp[-(a+b)^2] \frac{b}{a+b} \int_0^{+\infty} \frac{\exp(-t) dt}{t + 2ab + a^2} \left\{ 1 + \mathcal{O} \left[\frac{t}{(a+b)^2} \right] \right\} \\
&\rightarrow \exp(-b^2 - 2c) \int_0^{+\infty} \frac{\exp(-t) dt}{t + 2c} \\
&\rightarrow \exp(-b^2) \Gamma(0, 2c).
\end{aligned}$$

We are now ready to apply the results of equation (47) to equations (38) and (44) for $P(A, B)$ and $P(A, B, C)$, respectively. Keeping terms up to first order in δ_e and κ as well as terms proportional to $\delta_e \kappa$, we obtain

$$\begin{aligned}
P(A, B) \approx & \frac{\delta_{cd}}{2\pi S_d \sqrt{S_d S_e}} \exp\left(-\frac{\delta_e^2}{2S_e} - \frac{\nu^2}{2}\right) \left\{ 1 - \kappa + \frac{\kappa}{2} \exp\left(\frac{\nu^2}{2}\right) \Gamma\left(0, \frac{\nu^2}{2}\right) \right. \\
& \left. + \frac{\delta_e}{\delta_{cd}} \left[\nu^2 - 1 + \kappa - \frac{\kappa}{2} \exp\left(\frac{\nu^2}{2}\right) \Gamma\left(0, \frac{\nu^2}{2}\right) \right] \right\}, \quad (53)
\end{aligned}$$

$$\begin{aligned}
P(A, B, C) \approx & \frac{(\delta_{cp} - \delta_{cd}) \delta_{cd}}{[2\pi S_d (S_p - S_d)]^{3/2} \sqrt{S_e}} \exp\left(-\frac{\delta_e^2}{2S_e} - \frac{\nu^2}{2}\right) \\
& \times \left\{ 1 - \kappa + \beta \alpha \kappa - (1 - \alpha)^{3/2} \kappa \left[\sqrt{2\pi} \nu + \pi \exp\left(\frac{\nu^2}{2}\right) \operatorname{erfc}\left(\frac{\nu}{\sqrt{2}}\right) \right] \right. \\
& + \frac{\kappa}{2} \exp\left(\frac{\nu^2}{2}\right) \Gamma\left(0, \frac{\nu^2}{2}\right) + \frac{\delta_e}{\delta_{cd}} \left[\kappa + (1 + \beta \kappa \alpha)(\nu^2 - 1) + \sqrt{2\pi} \kappa \nu (1 - \alpha)^{3/2} (1 - \nu^2) \right. \\
& \left. \left. + \pi \kappa (1 - \alpha)^{3/2} \exp\left(\frac{\nu^2}{2}\right) \operatorname{erfc}\left(\frac{\nu}{\sqrt{2}}\right) - \frac{\kappa}{2} \exp\left(\frac{\nu^2}{2}\right) \Gamma\left(0, \frac{\nu^2}{2}\right) \right] \right\}, \quad (54)
\end{aligned}$$

in which

$$\nu \equiv \frac{\delta_{cd}}{\sqrt{S_d}}, \quad \alpha \equiv \frac{S_d}{S_p}, \quad \beta \equiv -2 + \frac{(1 - \alpha)^{3/2}}{2\alpha} \ln \left(\frac{1 + \sqrt{1 - \alpha}}{1 - \sqrt{1 - \alpha}} \right) + \frac{1}{\alpha} + 2\alpha. \quad (55)$$

Finally, using the results of equations (53) and (54), we reach the simplified expressions for $P(B|A)$ and $P(C|A, B)$ in equations (28) and (30) of §3.5.